

# Intensity and Time Resolved Scattered Laser Radiation Monitoring in Single Pulse Micro-Drilling as a Method for Quality Control

Roberto Ocaña<sup>\*1</sup>, Joseba Esmoris<sup>1</sup>, and Emeric Biver<sup>2</sup>

<sup>1</sup>*Tekniker, Basque Research & Technology, Eibar, Spain*

<sup>2</sup>*Multitel Innovation Centre, Belgium*

*\*Corresponding author's e-mail: [roberto.ocana@tekniker.es](mailto:roberto.ocana@tekniker.es)*

This paper presents a monitoring system for scattered laser radiation in the single pulse micro-drilling process. Scattered laser radiation is non-absorbed radiation scattered both at the surface and in the particles of the material removed. The system developed to measure this radiation is based on a fiber optic bundle attached to a narrow filter photodiode that captures the scattered light symmetrically around the area where the micro-drilling is performed. This provides sensitivity to non-symmetrical scattering processes (for example, in the event that the sample is tilted) and enables the system to be simplified by using only two photodiodes: One to monitor the beam entrance area and the other to monitor the beam exit. Two types of analysis are carried out on the two sides of the sample: Intensity monitoring and time resolved monitoring. The former can be used as a detector of deviations in the configured micro-drilling process and the latter as a real measurement of drilling time. A further analysis of these measurements enables correlations to be established with process parameters and physical scattering processes. The system designed is a low-cost tool for real-time quality monitoring of large, time-consuming industrial micro-drilling processes.

DOI: 10.2961/jlmn.2023.01.2003

**Keywords:** micro-drilling, monitoring micro-drilling, drilling time, drilling deviation detector

## 1. Introduction

In recent years, laser single pulse micro-drilling (SPMD) has established itself as a versatile technique that does not cause mechanical wear and is relatively simple to implement [1, 2]. This is why it is the technique most used in various industrial micro-drilling applications such as the development of Hybrid Laminar Flow Control structures in the aeronautical industry [3-6], jet fuel filtration [7], air water separation [8], particle sorting [9], audible noise reduction [10], etc. However, all these applications require reliable production of micro-holes with minimal failures, which in turn calls for control of hole diameters and overall quality. In fact, in extensive micro-drilling processes (for example in large areas or in repetitive production runs) deviations from the optimal conditions are common. They include formation of cumulative residual stresses in large pieces that bend the sample, deposition of the material extracted in the nozzle, which modifies the assist gas flow and absorbs energy from the laser beam, local deformations of the sample in the range of tens of microns, etc.

Perhaps one of the most common deviations during the processing of large samples is the loss of the configured working distance. Indeed, any change in the working distance can result in the production of areas with out-of-tolerance hole diameters. To avoid this problem, it is first necessary to have a system capable of measuring in real time the distance between the sample and the optical system with micrometric precision. Several methods have been proposed for this purpose, such as electromagnetic sensors [11], triangulation laser systems [12-13], capacitance sensors [14], etc. However, these methods are not completely reliable. For

example, in triangulation systems the measurement can fail when there are changes in the reflectivity of the surface due to inhomogeneities or an uneven mechanical finish. The electromagnetic and capacitance sensors are located very close to the sample and therefore are likely to become fouled by material ejected in the laser process, causing erroneous measurements. It is therefore necessary to supplement these sensors with further techniques that help either the operator or an automatic control to determine how accurate the measurement offered by the sensor is.

In recent years optical coherence tomography (OCT) [15] has established itself as the most appropriate method for measuring in real time the distance between the sample and the optical system. This technique is capable not only of working with the required precision but also of measuring in-situ, i.e. at the very location where the laser beam starts drilling. Drilling with OCT enables a closed loop control to be set with a travel stage for the height of the laser head operating at high rates in order to keep the working distance constant in the micro-drilling process. However, the use of OCT is not sufficient on its own to ensure a process free from deviations. As in the case of laser-based triangulation sensors, a local change in the reflectivity of the material (due to dirt or local oxidation, for example) might affect the measurement and send an incorrect working distance to the close loop control, thus leading the process to a different regime with different characteristics for the diameters and shapes of the micro-holes. For this reason, further in-situ monitoring techniques are needed to provide additional information on the laser process. Furthermore, OCT is a sophisticated, expensive measuring instrument that requires custom

adaptation of the laser head. Therefore, simpler monitoring techniques are also desirable.

Instead of monitoring a configuration parameter of the process, a different approach might be to measure one or more aspects of the physical phenomena involved. Such techniques include the monitoring of acoustic [16] and optical radiative effects [17]. In contrast to the monitoring of configuration parameters, measuring physical phenomena requires detailed analysis to correlate the measurements taken with the final results.

Photodiode monitoring of scattered laser radiation fits into the latter group of methods and is a simple technique that has proven feasible in various laser processes [18]. The sensing element is sensitive over a wide spectral range (300-1100 nm in Si, 800-1700 nm in InGaAs and 800-1800 nm in Ge photodiodes) and one or more sensors [19] arranged symmetrically can be used to capture the radiation from the process. To differentiate plasma formation and thermal radiation, broadband filters in the visible and near IR spectrums, respectively, are used [19]. However, in the case of thermal processes (>700 nm) the laser radiation scattered in the process (in the case of Nd:YAG and Yb:YAG lasers in the range of 1030 to 1070 nm), also contributes to the measurement. This can lead to incorrect analysis and interpretation of the results since the thermal effects are slower than the intensity variations in the scattered radiation. To avoid this problem, the contribution of thermal radiation is minimized in this study by using a narrow bandwidth filter at the laser wavelength. Thus, only the diffuse radiation produced when the laser beam hits the sample and the small amount of residual thermal radiation at the same wavelength can reach the photodiode. Furthermore, the energy radiated by heat accumulated is distributed in a wide spectrum defined by black-body Planck's Law, but the energy diffusely reflected by the sample is mainly concentrated at the laser wavelength. This means that the contribution of thermal effects to the radiation captured by the photodiode with filter is negligible and can be discarded in the analysis of the results. On the other hand, the diffusely reflected radiation is instantaneously correlated with the absorption of the laser beam and the amount of material removed participating in the scattering process. Thus, in contrast to the radiation produced by the thermal accumulation fundamentally linked to the pure absorption of the laser beam, this effect is closely related to fast and instantaneous aspects of the process and is therefore more appropriate for in-situ fast real-time monitoring.

In this study we have developed a system based on photodiodes and a fiber optic bundle that measures the instantaneous intensity of the scattered radiation of the laser and that can also be used to determine precise time-resolved aspects of the micro-drilling process. The analysis of the measurements enables correlations to be established with the diameters of the holes obtained, the volume of material removed in the micro-drilling process, and the position of the focusing optical system with respect to the sample.

## 2. Setup of the Experiment

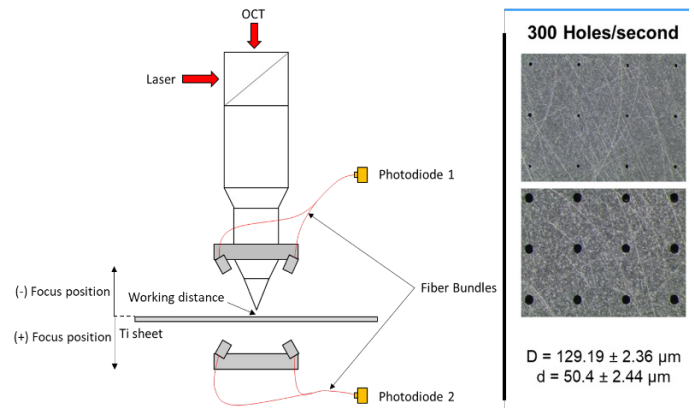


**Fig. 1** (Left) Schematic diagram of the setup of the experiment. (Right) Beam exit of a Ti sample micro-drilled with the single pulse drilling technique (Top) and beam entrance (bottom) where  $D$  is the mean diameter at the beam entrance and  $d$  at the beam exit

The left side of fig. 1 shows a schematic diagram of the setup for the experiment. The laser head is a conventional cutting head with a 100 mm focusing lens that can be adjusted (focus position) to place the beam waist at different positions with respect to the sample. The exact beam waist position with respect to the adjustment scale is measured with a scanning diagnostics system (Focus Monitor). The camera monitoring port available in the laser head is used in this case for monitoring with an OCT. The laser source is a QCW fiber laser with emission at 1070 nm and peak power 1.5 kW. Pulses are obtained by modulating the pumping diodes through an external signal provided by an FPGA. The pulses sent to the laser in the modulation signal are 200  $\mu$ s wide. The repetition rates of the pulses determine the drilling rate since one pulse produces a single micro-hole in the SPMD technique. The laser head is installed in a machine with axes that enable the working distance to be adjusted with micrometric precision and the head to be moved cross-wise over the sample to drill a defined area [20].

In this study, OCT is used to accurately measure the working distance in-situ. This system operates in spectral domain mode at a central wavelength of 930 nm with 2.9 mm imaging depth and 6  $\mu$ m axial resolution. The device is an instrument designed for 3D microscopy that is adapted to measure the distance between the head nozzle and the sample (working distance) by making use of the A-scans (difference in optical path between sample and reference arm). The internal sample rate is 3 KHz and custom-developed software is run on a computer for data processing. The measurement of optical path difference is then transferred to an analog output on a data acquisition board to establish controlling tasks. The sample rate on this output is a function of the processing capabilities of the computer and the characteristics of the data acquisition board. The sample rate was measured under real conditions and was found to be slightly higher than 800 Hz. This measurement is used by the automation control of a 3-axis machine [20] to perform a closed loop control through a PID algorithm that operates on the Z axis to keep the working distance constant with a  $\pm 5$   $\mu$ m error.

Experiments have shown that at working distances below 1 mm the laser head nozzle runs a certain risk of being

blocked by the material removed in the micro-drilling process. Hence, working distances greater than 1 mm are used in this study. On the other hand, as the head moves away from the sample, the carrying capacity of the assist gas in removing the material decreases, as does the overall quality of the holes. Therefore, an acceptable range in our experiment for the working distance that enables work to take place with no risk of blocking the nozzle and minimizing burrs in the holes is from 1 mm to 1.2 mm. Fig 1 shows the working distance and the adjustment of the beam waist (focus position).

To monitor the scattered laser radiation at the beam entrance and exit, two Si photodiodes with narrow filters (3 nm) at the wavelength of the processing laser (1070 nm) are used. This enables us to capture just the scattered radiation of the processing laser and to discard any other contribution (plasma, heat, etc.). Si photodiodes are known for sharp decreases in sensitivity above the visible spectral range. However, at the narrow wavelength interval of the processing laser, this is 0.35 A/W or 40% of the maximum sensitivity. The photodiode and narrow filter assembly are attached to a 4:1 fiber optic bundle with a 600 μm core. Each end of the fiber is then protected with an optical window and placed symmetrically around the laser head aimed at the process zone by means of a custom piece built with rapid prototyping as shown on the left side of fig.1. This piece contains interior channels that conduct pressurized N<sub>2</sub> to the surface of the windows in order to avoid deposition of particles from the process or from the environment.

As indicated on the right side of fig. 1, the productivity of the SPMD technique on 0.8 mm Ti sheet is 300 holes per second [2, 20, 21]. The micro-holes are measured by a custom artificial vision system that works off-line and enables us to establish a correlation between the dimensions and quality of the drills and the in-situ monitoring measurements. The CMOS camera of the vision system uses the axis of the laser system itself to position the camera over the sample surface. The lens installed captures an area of 4.9 x 4.9 mm<sup>2</sup> at the sample surface at 100 Hz. Several holes can be measured at the same time by a custom-developed machine vision algorithm. This system can provide measurements of the beam entrance diameter, circularity, area, effective pitch and clogged holes. To measure the diameter of the holes, the system takes two types of measurement on the micro-holes detected and then calculates the average. The first measurement type is the maximum Feret diameter. This is the module of the line segment that connects the two perimeter points that are the furthest apart, i.e.

$$d_{Feret} = \sqrt{(F_{y2} - F_{y1})^2 + (F_{x2} - F_{x1})^2}, \quad (1)$$

where  $F_{y2}$  is the  $y$  coordinate of the end point,  $F_{y1}$  is the  $y$  coordinate of the start point,  $F_{x2}$  is the  $x$  coordinate of the end point and  $F_{x1}$  is the  $x$  coordinate of the start point. The second type of measurement is the Waddel Disk diameter. This measures the diameter of a disk with the same area ( $A$ ) as the micro-hole detected, i.e.

$$d_{Waddel} = 2 \sqrt{\frac{A}{\pi}} \quad (2)$$

The reason why these two types of measurement of the micro-hole diameter are averaged is to take into account the circular symmetry of the micro-holes but at the same time to allow a degree of freedom for any deviations from circular symmetry. Thus, the average is a convolution of these two concepts and deviations from circular symmetry influence the dispersion of the measurement.

### 3. Results

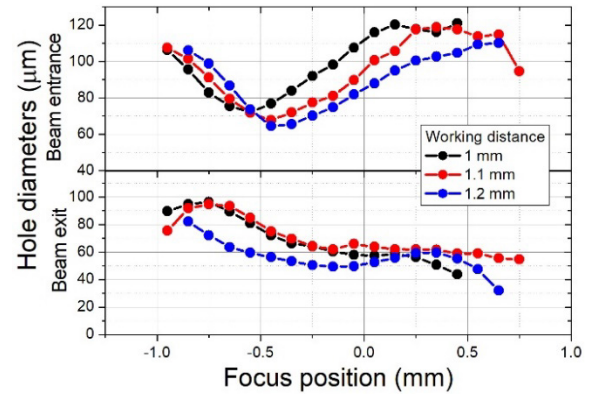


Fig. 2 Diameters of the micro-holes measured by the custom machine vision system as a function of the beam waist position of the laser beam at three different working distances. (Top) Beam entrance diameter. (Bottom) Beam exit diameter

In order to study the complete range of micro-hole diameters that can be obtained with the SPMD process, Ti samples (0.8 mm thick) with 300 micro-holes processed at different working distances and beam waist positions were made under controlled conditions using the OCT. To characterize the micro-holes made with the SPMD technique we use the artificial vision system described above to measure hole diameters. Working distance and beam waist position are the parameters most sensitive to deviations due to the difficulty in controlling the micro-drilling process on large samples with micrometric precision. The results are shown in fig. 2. Each point in this figure represents the mean diameter measured by the machine vision system automatically. The maximum dispersion found in the diameters is  $\pm 10 \mu\text{m}$  for the beam entrance and  $\pm 5 \mu\text{m}$  for the beam exit. Below -0.95 mm and above 0.75 mm focus position the dispersion increases significantly because some holes are not completely drilled. This indicates a low level of stability and reproducibility of the process in these regions. As shown in fig. 2, the beam exit diameter increases when the beam waist is brought up (from bottom to top), but the beam entrance diameter shows a minimum. The focus position 0 mm represents the position of the beam waist at the top surface of the sample for the 1.2 mm working distance. This position however does not coincide with the minimum beam entrance for this sample thickness. In fact, the formation of the hole diameter is a complex process in which not only the spot diameter of the laser beam but also the dynamics of the energy absorbed by the sample and the flow and pressure of the inert assist gas play important roles [21]. The curves in fig. 2 show that there are areas with different levels of sensitivity to deviations at the beam entrance or exit due to non-negligible

slopes beyond the maxima and minima. For most points, a deviation of just 0.1 mm in the working distance or in the position of the beam waist with respect to the sample can significantly change the diameters obtained. Therefore, it is important to ensure the working distance and position of the beam waist relative to the sample for a chosen diameter pair by means of monitoring tools. OCT is sensitive to both working distance and the position of the focusing lens of the optical system but insensitive to other effects. For example, if the head nozzle becomes dirty the gas assist flow might change, and OCT would not detect any deviation. In fact, any deviation in the gas assist flow or in the power of the laser beam would go undetected by OCT, placing the diameters and characteristics of the micro-holes outside of tolerances. This in-situ monitoring technique therefore needs to be supplemented by further tools that make up for this lack of information.

The molten material is ejected by an Ar flow at 18 bar coaxially with the laser beam. Together with the shape of the laser beam around the beam waist, this produces micro-holes that are not perfectly conical [21]. Nevertheless, as a first approach, it is possible to estimate the volume of material removed as a truncated cone as follows:

$$V = \frac{1}{3} \pi t (d_e^2 + d_x^2 + d_e d_x), \quad (3)$$

where  $t$  is the sample thickness and  $d_e$  and  $d_x$  are the diameters at the beam entrance and exit respectively. This is shown at the bottom in fig. 4. As expected, for most beam waist positions, the material extraction capacity of the micro-drilling process decreases as the head moves away from the sample and the volume of the micro-holes becomes smaller. This can be explained by taking into account that the farther the nozzle is from the sample, the larger the turbulent effects in the assist gas flow are, and therefore the smaller the capacity to drag the molten material is.

All curves in the bottom graph of fig. 4 show a minimum and a rapid growth of the removed material as the position of the beam waist is changed. This position with minimal material removal is reached when the beam waist is slightly above the top surface of the sample for each working distance.

### 3.1 Time-resolved measurements

The experiment set up as per in fig.1 enables us to measure time-dependent characteristics of the process by simultaneously using the top and bottom scattering monitoring systems. Unlike amplitude measurements, time-resolved measurements can provide an insight into the temporal dynamics of the process without being affected by eventual sensitivity changes of the measurement tool. That is why this type of monitoring is more appropriate when a fixed relationship between the physical phenomenon and the signal produced by the sensor cannot be guaranteed in time-consuming processes. Thus, for example, if an optical protection window becomes dirty, a system based on amplitude measurements will show less intensity while a time-resolved measurement will continue to give reliable measurements as long as the signal to noise ratio is high enough.

In order to determine the time-dependent characteristics of the SPMD process, the following procedure was

developed: The monitoring system at the top of the sample detects the time at which the laser beam reaches the sample, and then the lower system measures the time elapsed until the sample is penetrated by detecting scattered radiation from the laser at the bottom of the sample.

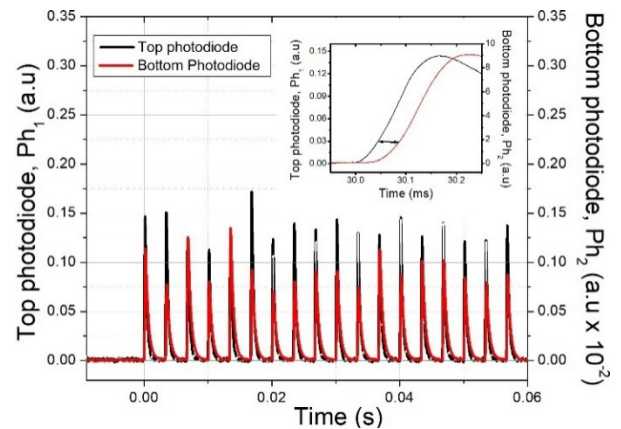


**Fig. 3** Signals captured with the top and bottom photodiodes during 60 ms working at a production rate of 300 holes/s at -0.75 mm focus position and 1mm working distance. The inset shows a close-up of the signals for the hole that is started at  $t=0.30$  s. The arrow in the inset shows the point at which delay is measured using the criteria defined in the text.

Fig. 3 shows the signals captured by the top and bottom monitoring systems. To extract the drilling time from these signals a criterion must be established. We have chosen the difference in time between the points on the rising edge of the curves at 20% of the peak height. This is indicated by the arrow in the inset in fig.3. This calculation can be implemented in real time using software or hardware. In our experiment it was done with a Matlab script associated with two analog inputs on a data acquisition board. Obviously, this is not the total drilling time since the hole is formed throughout the duration of the laser pulse (200  $\mu$ s) but it provides the time necessary for the laser beam to reach the lower surface of the sample. Therefore, the drilling time is a function of the amount of material to be removed from the sample, so it should correlate with the shape and volume of material removed.

Fig. 4 shows the drilling time defined as a function of the position of the beam waist at different working distances. The curves resemble the non-monotonic dependence of the model to estimate the material removed and demonstrate that the drilling time is correlated with the shape of the holes. Therefore, if the working distance and position of the beam waist are configured to obtain a certain pair of diameters for the beam entrance and exit, a drilling time given by the curves of the upper graph in the fig. 4 should be measured in-situ. A deviation in the average drilling time would mean that a process parameter has changed and hence, the diameters and shapes of the holes would be expected to be different as well. The curves in fig. 4 could be used as training inputs in the framework of a control strategy via machine learning or as a lookup table within a conventional control approach for real-time monitoring of diameters and overall quality of the micro-drilled sample.

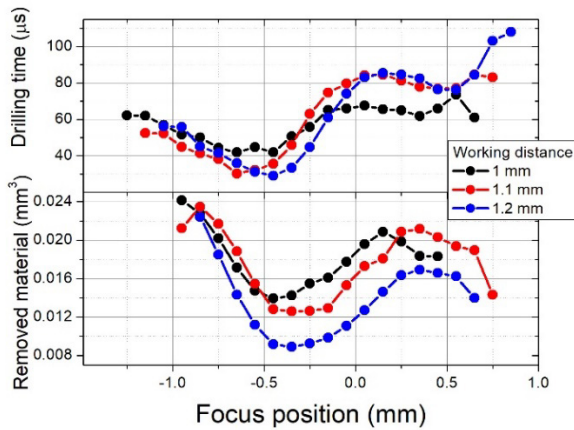


Fig. 4 (Top) Drill-through time measured by the photodiodes as function of focus position at three working distances. (Bottom) Estimation of the material removed in the micro-drilling process obtained from the diameters at the entrance and exit of the beam and a model for the volume in the form of a truncated cone.

Fig. 4 also shows that the variation of the drilling time as function of the beam waist position is greater in the case of working distances 1.1 and 1.2 mm. This indicates a greater sensitivity to deviations in the areas beyond maxima and minima (points with no sensitivity to deviations). Therefore, if an adequate combination of diameters for the beam entrance and exit can be found for a certain application, it is preferable to choose greater working distances. This would provide more sensitivity to deviations in regions with non-zero slope. By contrast, if lower susceptibility to changes in diameter due to eventual deviations is required, less sensitivity in drilling time should be expected as a drawback. In fact, these regions coincide with those that show almost zero slope in the material removed curves. Figs. 2 and 3 provide an overview of the diameters achievable and the sensitivity of the drilling process to deviations, and an insight into the potential performance of a drilling time control. Depending on the need to implement a real-time control strategy for a given application and the requested hole specifications, a specific region from the curves is chosen to minimize the effect of potential deviations.

### 3.2 Intensity-resolved measurements

As explained in the previous section, unlike time-resolved measurements, amplitude measurements depend on the effective sensitivity of the capture system. This sensitivity can be reduced by dirt accumulated on the optical fiber protection windows. Indeed, in applications that require micro-drilling of large samples with processes lasting tens of hours, the material removed in the process might deposit on the optical surfaces dedicated to inspection and monitoring. The solution to this problem is to implement a blowing system that prevents dust deposition and keeps surfaces clean. In our setup, the piece that supports the four fibers and the optical protection windows is manufactured by rapid prototyping and designed with internal microchannels that conduct high-pressure nitrogen. The flow of nitrogen over the optical window surfaces keeps them clean and prevents

deposition of particles and material. Another effect that could influence a monitoring strategy regarding amplitude measurements is the tilting of the sample. In fact, when a sample is drilled with a large number of micro-holes, the stresses induced in the formation of each hole tend to bend the Ti sheet. To avoid this, the custom micro-drilling system developed [20] contains elements and fixtures that keep the sheet perpendicular to the laser beam. In any case, the influence of sample tilt on the capture of the scattered radiation is integrated through symmetrical monitoring with the 4 fibers around the laser beam at the top and bottom of the sample. Therefore, if such a deviation occurs in the process, the system will detect it. Nevertheless, in this study, this effect has been controlled for and can be completely ruled out when analyzing the results. As explained above, deviations in the micro-drilling process are more likely to appear due to the micrometric precision required for positioning the laser head in the direction perpendicular to the sample.

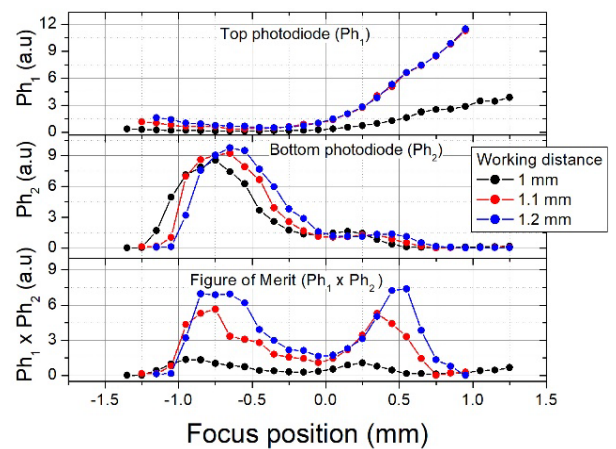


Fig. 5 (Top and center) Signal captured by the top ( $Ph_1$ ) and bottom ( $Ph_2$ ) photodiodes respectively as a function of the focus position. (Bottom) Merit function  $Ph_1 \times Ph_2$  calculated, defined as an overall identifier of the scattering distribution.

Fig. 5 shows the amplitude of the signal captured by the top ( $Ph_1$ ) and bottom ( $Ph_2$ ) monitoring systems as function of the beam waist position at the same working distances used previously. As shown, the scattered radiation at the top of the sample decreases when moving the beam waist up, but the bottom scattered radiation increases and shows a maximum. This maximum also coincides with the region where the material removed increases (see fig.4). This means that at these focus positions more molten material is expelled at the beam exit, dragged by the high-pressure assist gas, so this material in the form of particles is likely to produce more scattering of the laser beam. For larger beam waist positions, a slight increase in the scattering at the top and a decrease at the bottom are again observed, indicating a redistribution in the way the material removed is ejected.

The redistribution of the laser beam scattering at the top and bottom of the sample depending on the position of the beam waist can be analyzed from a more general approach. In fact, if a merit function is defined as the multiplication of the two signals ( $Ph_1 \times Ph_2$ ) in order to include the two monitoring systems at the same time, a quasi-symmetric curve

centered at the focus range from -0.3 to 0 mm depending on the working distance with two maxima at both sides is observed. The 0mm position is defined as the position where the beam waist is at the top surface of the sample for a 1.2mm working distance. In the case of a 1 mm working distance, the beam waist is at the top of the sample when the -0.2 mm focus position is set. Hence, with this analysis it is possible to determine the point where the scattering of the laser begins to be more significant at the top or bottom of the sample. At the same time, the redistribution of the scattering as the beam waist is moved through the sample shown in the defined figure of merit serves both to determine in-situ the beam waist position without further measurement tools and to identify potential deviations from the starting conditions set in industrial applications requiring large micro-drilled surfaces.

#### 4. Conclusions

In this study we present a real-time, low-cost, in-situ monitoring system for the single-pulsed micro-drilling process. This monitoring system is based on sensing the scattering of the laser beam by means of photodiodes with narrow bandwidth filters around the laser wavelength and fiber optic bundles arranged symmetrically in the area of the beam entrance and exit. This enables us to perform both an amplitude analysis and a time-resolved study of the laser scattering processes and thus rule out the influence of thermal effects on the measurement. The data collected shows that there is a relationship between the signals from the sensors, the diameters of the drilled holes at the beam entrance and exit and the volume of material removed. Furthermore, novel information can be drawn from the laser process about the position of the beam waist relative to the sample, the distribution of the scattering on both sides, hole formation and the relevant direction of ejection for the material removed. These systems can thus be used in simple processes within the framework of control tasks as real-time detectors of deviations or as a supplementary monitoring method within more highly-developed approaches such as closed-loop controls with OCT to ensure quality and compliance with application specifications.

#### Acknowledgments

This work was funded by the European Union's Horizon 2020 research and innovation program under Grant Agreement No 825567.

#### References

[1] J. Cheng, W. Perrie, M. Sharp, S. P. Edwardson, N. G. Semaltianos, G. Dearden, and K. G. Watkins: *Appl. Phys. A*, 95, (2009) 739.

- [2] A. Stephen, R. Ocaña, J.I. Esmoris, C. Thomy, C. Soriano, and F. Vollertsen: *Procedia CIRP*, 74, (2018) 403.
- [3] S. Williams: "Laser drilling of porous panels for laminar flow control" ed. by C. Webb, and J. Jones, (CRC Press, London, 2004) p.1648.
- [4] C. Y. Yeo, S. C. Tam, S. Jana, and M. W. S Lau: *J. Mater. Process. Technol.*, 42, (1994) 15.
- [5] T. Young, B. Mahony, B. Humphreys, E. Totland, A. McClafferty, and J. Corish: *Aerosp. Sci. Technol.*, 7, (2003) 181.
- [6] G. Schrauf: *Aeronaut. J.*, 109, (2005) 639.
- [7] X.S. Zhang, Z.Y. Zhang, H. Zhu, S.W. Li, Y. F. Wang, K. Xu, S.L. Chu, and J.J. Huang: *Lasers Eng.*, 52, (2022) 37.
- [8] S.Ye, Q. Cao, Q. S. Wang, T.Y. Wang, and Q. Peng: *Sci. Rep.*, 6, (2016) 37591.
- [9] R. Y. Wang, P. C. Wu, Z. Zhang, B. Xu, Y.L. Hu, W. Zhu, J. Li, J. Chu, D. Wu, and G. Li: *Opt. Eng.*, 57, (2018) 056114.
- [10] P. Wu, S. Ji, T. Cao, Y. Li, X. Li, and Y. Li: *IEEE Trans. Power Deliv.*, 24, (2009) 1756.
- [11] R. Ocaña, I. Garmendia, and C. Soriano: *Proc. SPIE*, 10683, (2018) 1068303.
- [12] S. Donadello, M. Motta, A. Gökhan Demir, and B. Previtali: *Opt. Lasers Eng.*, 112, (2019) 136.
- [13] T. Purtonen, A. Kalliosaari, and A. Salminen: *Phys. Procedia*, 56, (2014) 1218.
- [14] A. Topkaya, K.-H. Schmoll, and R. Majoli: *Proc. SPIE*, 1024, (1989) 103.
- [15] M. Kogel-Hollacher, S. André, and T. Beck: *Proc. SPIE*, 10911, (2019) 109110F.
- [16] A. Papanikolaou, G.J. Tserevelakis, K. Melessanaki, C. Fotakis, G. Zacharakis, and P. Pouli: *Opto-Electron. Adv.* 3, (2020) 190037.
- [17] M. S. Rabasović, D. Šević, N. Lukač, M. Jezeršek, J. Možinaand, and P. Gregorčič: *Appl. Phys. A*, 122, (2016) 186.
- [18] C. Bagger and F. Olsen: *J. Laser Appl.*, 15, (2003) 19.
- [19] S. M. Garcia, J. Ramos, I. Arrizubieta, and J.Figuera: *Appl. Sci. (Basel)*, 10, (2020) 6556.
- [20] C. Soriano, A. Arizaga, R. Ocaña, M. Sanchez, A. Stephen, R. Sanchez, and L. Uriarte: *Dyna*, 96, (2021) 130.
- [21] R. Ocaña, C. Soriano, J. Esmoris, and R. Sánchez: *J. Laser Micro Nanoeng.*, 14, (2019) 54.

(Received: June 24, 2022, Accepted: January 19, 2023)